



Synthesis and characterization of ZnO nanoparticles at different molarity concentrations for photocatalytic applications

S.V. Elangovan^{a,*}, V. Chandramohan^b, N. Sivakumar^c, T.S. Senthil^d

^aDepartment of Chemistry, Velalar College of Engineering and Technology, Erode, India, Tel. +91 9788624951; email: kanjielango@gmail.com

^bDepartment of Chemistry, P.S.G. College of Arts & Science, Coimbatore, India, Tel. +91 9043904930; email: chandramohanphd@gmail.com

^cDepartment of Chemistry, Chikkanna Govt. Arts College, Tiruppur, Tamilnadu, India, Tel. +91 9865302003; email: sukisivakumar@gmail.com

^dDepartment of Physics, Erode Sengunthar Engineering College, Erode, India, Tel. +91 9944639993; email: tssenthi@gmail.com

Received 5 August 2014; Accepted 17 March 2015

ABSTRACT

Zinc oxide (ZnO) nanocrystals were synthesized under three different molarity concentrations by simple wet chemical method. The prepared ZnO nanocrystals are annealed at 250, 350, and 450 °C. The X-ray diffraction results show that the crystallinity has been observed to improve on annealing. The effect of annealing and molarity concentrations on structural and optical property, and surface morphology of ZnO nanocrystals were analyzed. The photocatalytic activity of synthesized ZnO nanocrystal has been investigated for methylene blue dye. The irradiation time, pH conditions of the synthesized ZnO nanocrystals were taken into account for the photocatalytic degradation process.

Keywords: ZnO nanocrystals; Wet chemical method; Surface morphology; Photocatalytic activity

1. Introduction

Many small and large scale industries such as textile, paper and pulp, plastic, and dyestuff industries consume large quantity of water and chemicals for various processes. The textile industry is one of the primary consumers of dyes along with large number of secondary chemicals for dyeing, printing, and finishing processes. The treatment of industrial effluents is to reduce or remove coloring agents and dissolved organic contaminants to meet environmental demands, which also attract the interest of research groups.

Many conventional and non-conventional methods are existing and emerging to remove pollutant materials from wastewater, but they create pollutant in another form. Hence, there is an intension to find an alternative cost-effective method. One such method is using inorganic oxides as photocatalyst.

A large number of inorganic nanomaterials such as TiO₂, zinc oxide (ZnO), CdSe, WO₃, PbSe, and PbS are used as electron acceptors for variety of applications [1]. Among them ZnO has special chemical and physical properties, with the advantages such as non-toxicity, low-cost, and easy fabrication [2]. It is also an important semiconductor with a wide direct band gap of 3.37 eV and large exciton binding energy of 60 meV

*Corresponding author.

at room temperature [3–5]. It is known that ZnO nanomaterial can be made with the most diverse and abundant configurations of nanostructures such as quantum dots, rods, wires, belts, springs, bows, helices, and prisms. ZnO nanomaterials with variety of structures can be prepared by different methods and fine particles of the oxide, which have decolorization and antibacterial action. For photocatalysis, ZnO has also been considered as a suitable alternative for TiO₂ due to its similar band gap and lower cost [6]. Moreover, it exhibits better performance in the degradation of organic dye molecule in both acidic and basic media.

Due to this, ZnO nanoparticles are added into various materials including cotton fabric, rubber, and food packaging. It has wide applications in medical field to cure different skin conditions, in products such as baby powder and barrier creams to treat diaper rashes, and in calamine cream, antidandruff shampoos, and antiseptic ointments. Zinc oxide is used as an important semiconducting material for various applications such as photoelectric, photocatalysis, piezoelectric devices, electroluminescence, nonlinear optical devices, light-emitting diodes, lasers, strain sensors, surface switches, and other nanodevices [7–15]. Many deposition techniques have been employed to prepare ZnO nanostructures, such as chemical vapor deposition, sol–gel method, sputtering deposition, and chemical solution deposition [16–19]. Out of these methods, the sol–gel technique has many advantages such as simple, inexpensive, non-vacuum, and room temperature process. This method offers many advantages such as homogeneity, stoichiometry and purity can be easily achieved, ease of processing and control of composition, and ability to prepare in large volume. One unique property of sol–gel process is the ability to go all the way from the molecular precursor to the product, allowing a better control of the whole process, and the synthesis of tailor made materials for various applications. In the present study ZnO nanocrystal has been prepared by the simple sol–gel method at room temperature. The synthesized nanocrystals are annealed at three different temperatures and are characterized by different techniques.

2. Experimental

2.1. Materials

AR grade of Zinc acetate, sodium hydroxide, and methylene blue were purchased from Merck specialties private Limited, Mumbai and used without further purification. All solutions were prepared with double distilled water.

2.2. Catalyst preparation

Zinc oxide nanoparticles were synthesized by wet chemical method using zinc acetate and sodium hydroxide precursors. In this experiment, 0.5, 1, and 1.5 M aqueous solution of zinc acetate Zn(CH₃COO)₂·2H₂O was kept under constant stirring using magnetic stirrer to dissolve completely. 0.5, 1, and 1.5 M aqueous solution of sodium hydroxide (NaOH) were also prepared in the same way with stirring of 20 min. After complete dissolution, NaOH aqueous solution was added drop by drop under vigorous stirring of zinc acetate solution. The reaction was allowed to proceed for 4 h after complete addition of NaOH. After the completion of reaction, the solution was allowed to settle for overnight and further, the supernatant solution was separated carefully. The remaining solution was centrifuged for 10 min, and the precipitate was removed. Thus, precipitated ZnO nanoparticles were cleaned several times with deionized water to remove the byproducts, which were bound with the nanoparticles and then dried in air atmosphere at about 70°C for 1 h. Finally the synthesized nanoparticles were annealed at three different temperatures such as 250, 350, and 450°C. During drying, Zn(OH)₂ is completely converted into ZnO nanoparticles.

2.3. Characterization

The prepared ZnO nanoparticles were characterized by X-ray diffraction (Rigaku D max-C) with Cu K α radiation (1.5406 Å). Morphology and composition of the synthesized samples were investigated using scanning electron microscope (SEM with EDXA, Sirion). The optical absorption spectra of ZnO nanoparticles were recorded using a UV–vis spectrophotometer (JASCO V-570).

2.4. Photocatalytic experiments

In wastewater large number of hazardous organic compounds are present. Among them methylene blue is one of the familiar organic dyes and causes serious environmental problems. Because of this, we selected methylene blue as a model sample to evaluate the photocatalytic activity of the synthesized nanocrystals. The photocatalytic experiments were carried on the catalysts sample prepared using 1 M concentration and annealed at 350°C. The rate of decolorization was recorded with respect to the change in the intensity of absorption peak in visible region. At the given time interval, the solution was withdrawn from the reactor and centrifuged and filtered through a Millipore filter

to remove the photocatalyst. Then, pH of the solution was adjusted using 0.1 N H_2SO_4 (or) 0.1 N NaOH and required amount of photocatalyst (0.25 g L^{-1}) was added into the vessel. The filtrate was analyzed by UV–visible spectrophotometer at $\lambda_{\text{max}} = 668 \text{ nm}$ to evaluate the residual MB concentration. The decolorization efficiency was defined as follows:

$$\text{Photodegradation (\%)} = (C_0 - C)/C_0 \times 100 \quad (1)$$

where C_0 is the concentration of MB before irradiation ($t = 0$) and C is the concentration of MB after a certain irradiation time [20].

3. Results and discussion

3.1. X-ray diffraction

To identify the crystal structure and growth orientation of the ZnO nanostructures X-ray diffrac-

tion studies have been carried out. Fig. 1 shows the X-ray diffraction pattern of the ZnO nanocrystals prepared using (a) 0.5 M, (b) 1.0 M, and (c) 1.5 M and annealed at different temperatures. The result reveals that the prepared samples are hexagonal wurtzite structure and it does not contain any characteristics peaks other than ZnO peaks, which confirm that the synthesized nanoparticles are free from impurities. The diffraction peaks at 2θ (degree) of 31.98, 34.57, 36.25, 36.39, 47.7, 56.7, 62.9, and 68.51 are, respectively, indexed to (1 0 0), (0 0 2), (1 1 1), (1 0 1), (1 0 2), (1 1 0), (1 0 3), and (2 0 1) planes of ZnO. They are in good accordance with the JCPDS card No. 36-1451. The average grain size of the samples was estimated with the help of Scherrer formula, $D = 0.89 \lambda / (\beta \cos \theta)$, where λ is the wavelength (Cu $K\alpha$), β is the full width at half-maximum (FWHM), and θ is the diffraction angle.

For 1 M concentration, the calculated grain size values are 23.3, 23.7, and 31 nm for 250, 350, and

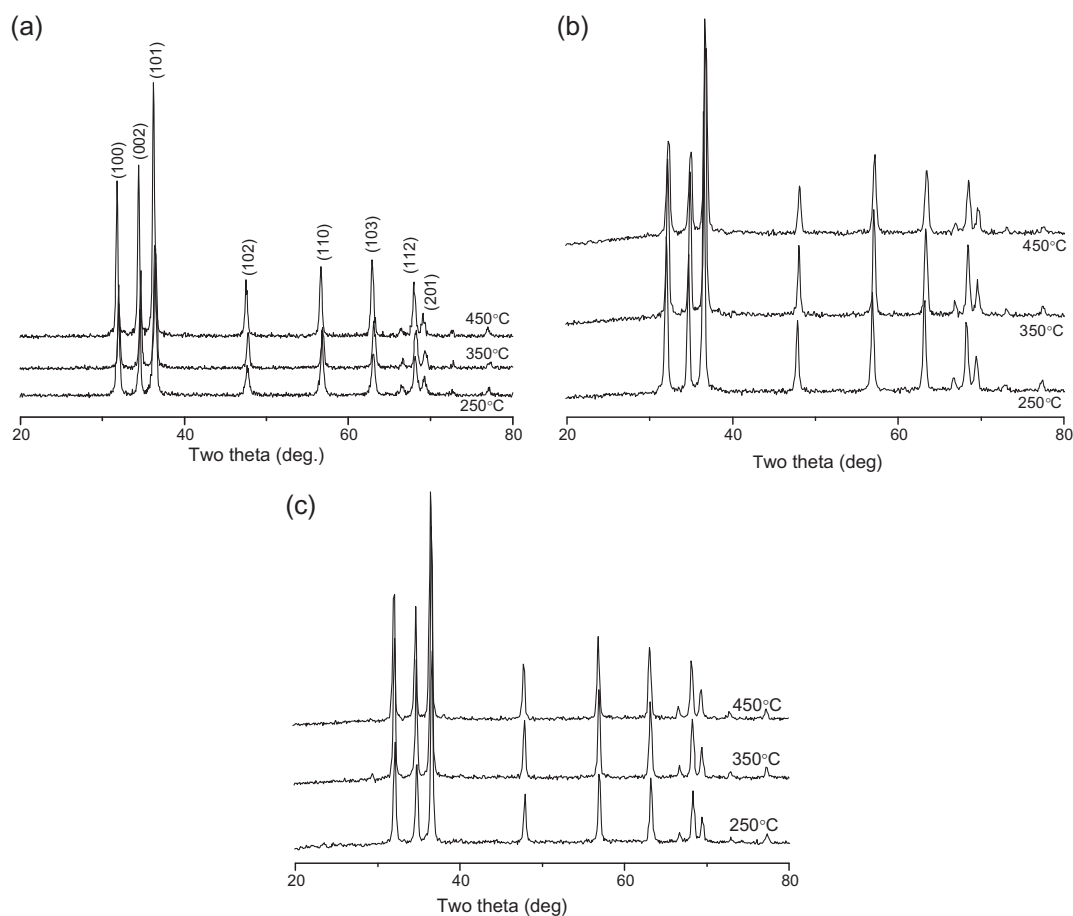


Fig. 1. X-ray diffraction pattern of ZnO nanocrystals prepared using (a) 0.5 M, (b) 1.0 M, and (c) 1.5 M and annealed at different temperatures.

450 °C, respectively, with respect to (1 0 1) plane. For all the mole concentrations when the reaction temperature increases, FWHM decreases. Thus the size of ZnO nanoparticles increases with the increase in temperature. This is due to the change of growth rate between the different crystallographic planes [21].

3.2. SEM and EDXA

Fig. 2(a)–(c) shows the SEM images of ZnO nanoparticles synthesized using 0.5 M and annealed at 250, 350, and 450 °C, respectively. From the SEM analysis it was clearly found that the prepared samples are in nanometer size and the surface morphology changes with temperatures. When the temperature increases, the particles get agglomerated and particle size increases. Also when the concentration and the annealing temperature increased the shape of the nanoparticles are changed into nanorods.

When the ZnO concentration is 1.5 M and annealing temperature is 250 °C, the obtained images are small and spherical in shape. For the same concentration when temperature increased to 450 °C, the morphology gets changed into wire-like structure. The reason for the increase in particle size is at higher concentrations, the alkalinity is increased, and this increase in alkalinity favors growth mechanism. The higher concentration increases the pH of the precursor solution and thereby enhances the crystal growth. Due to this the particle size increases with the increase in solution concentration.

Energy dispersive X-ray analysis (EDXA) is based on the principle of unique atomic structure, which provides unique set of peaks on its X-ray spectrum for each element. Fig. 3, shows the EDXA pattern of ZnO nanoparticles synthesized using 1 M and annealed at 350 °C. From the spectra it was identified that all the prepared samples contain only Zn and O elements

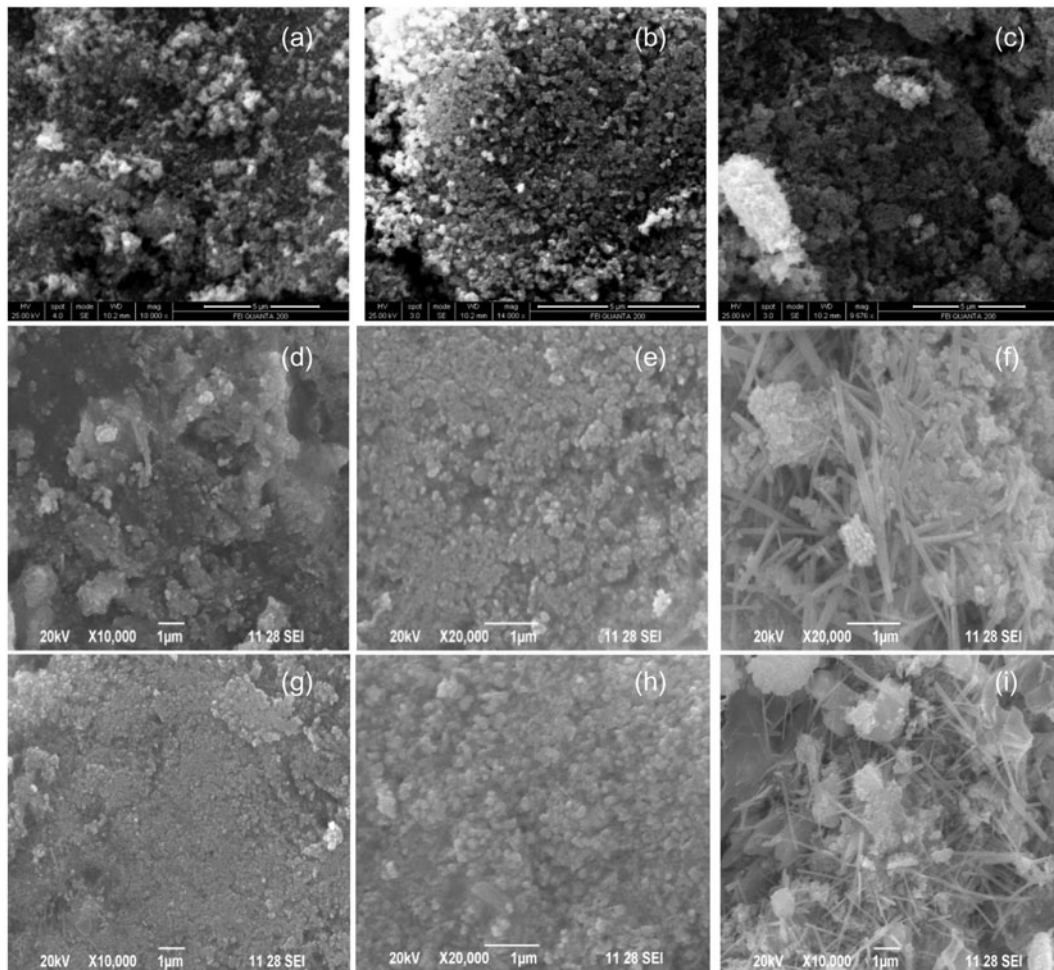


Fig. 2. SEM images of ZnO nanocrystals synthesized using ((a)–(c)) 0.5 M, ((d)–(f)) 1 M, and ((g)–(i)) 1.5 M and annealed at 250, 350, and 450 °C, respectively.

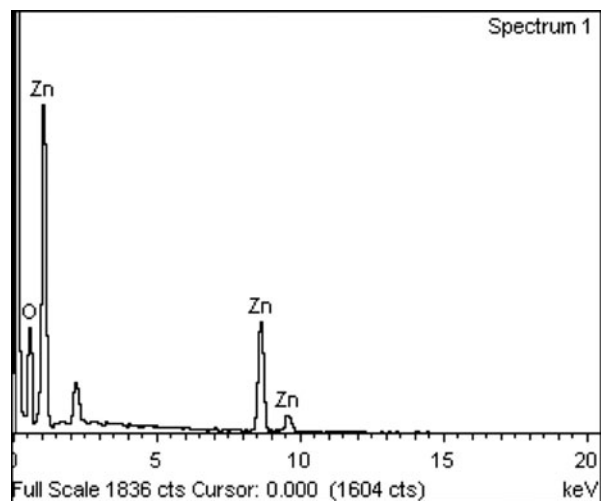


Fig. 3. EDXA spectrum of ZnO nanoparticles synthesized using 1 M and annealed at 350°C.

and no other elements were detected. So, the synthesized samples are free from impurities. The unidentified peaks at 2.2 keV is due to the presence of platinum. The origin of platinum is from the platinum coating on the nanoparticles.

3.3. UV–vis spectra

UV–visible spectroscopy is mainly used to identify the optical characteristics of synthesized nanoparticles. Fig. 4 shows the absorbance spectra of ZnO nanocrystals synthesized using different molarity concentrations and annealed at different temperatures. All the samples show a good absorbance in the wavelength range of 325–350 nm, after that a sharp decrease in absorbance is found. It seems that variation in the absorbance is due to variation in the synthesis conditions such as annealing temperature. An excitonic peak is identified for individual mole concentration

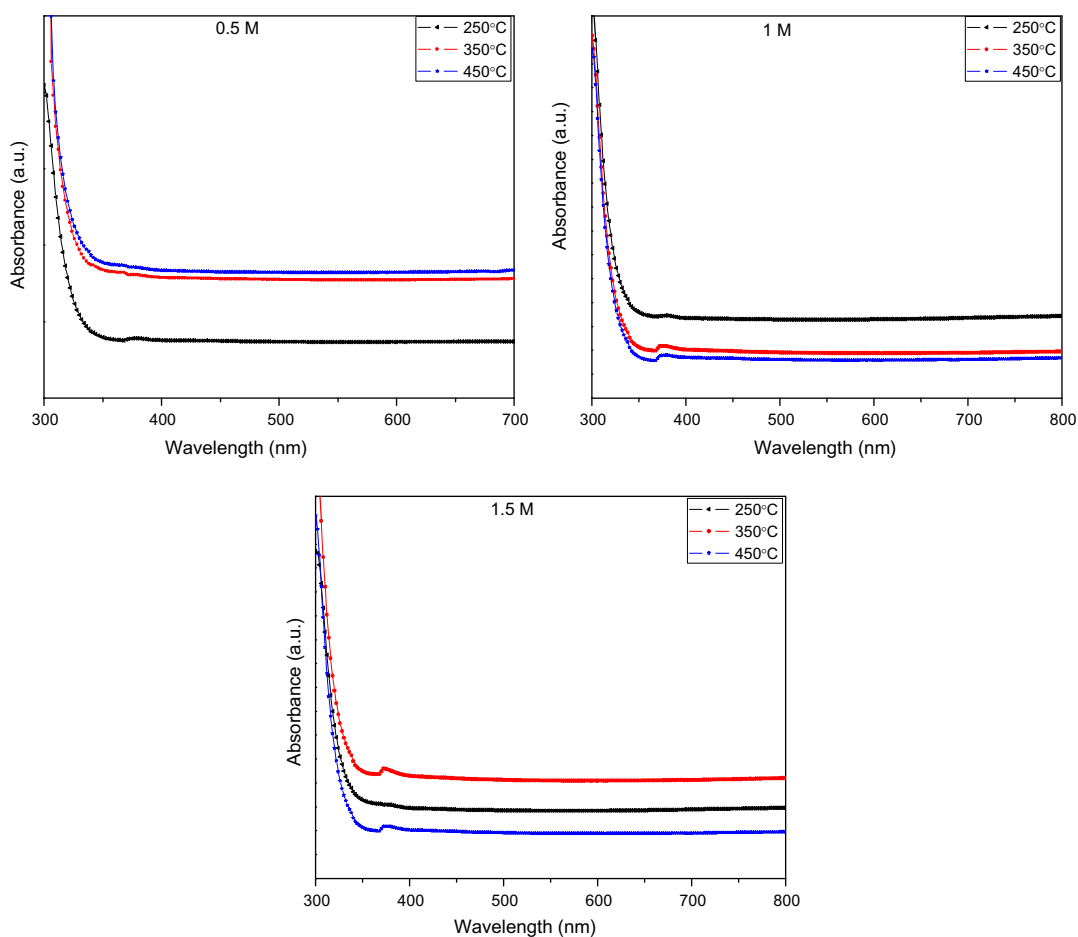


Fig. 4. Absorbance spectra of ZnO nanocrystals synthesized using different molarity concentrations and annealed at different temperatures.

Table 1
Band gap value of the synthesized ZnO nanocrystals

Annealing temperature (°C)	Band gap for different molarity concentrations (eV)		
	0.5 M	1 M	1.5 M
250	3.74	3.78	3.79
350	3.65	3.69	3.70
450	3.55	3.56	3.57

and annealing temperature and their wavelength values are in the range of 327–350 nm. The band gap energy (E_g) of synthesized zinc oxide nanocrystals are calculated by using the intercept of the tangent to the x-axis from plots of wavelength vs. absorbance. The obtained values are tabulated in the Table 1. The band gap values did not show much difference, though particle size varied due to the increase in ZnO concentration and annealing temperature. A ZnO nanoparticle with a wide band gap of 3.37 eV, a peak is expected to be at 358 nm. Graph indicates that there is a strong blue shift in the absorption spectra of ZnO nanocrystals and particles are smaller than the Bohr radius of exciton for ZnO nanoparticles.

4. Photodegradation of MB

4.1. Effect of pH

The adsorption of dye molecules on ZnO nanoparticles strongly depends on the pH of the solution. The effect of pH on the photodegradation of MB dye was studied by varying the pH of the solution

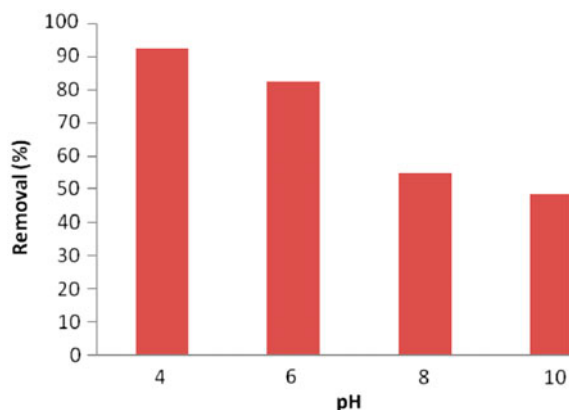


Fig. 5. Effect of pH on the photodegradation of MB.

from 4 to 10. The results are displayed in Fig. 5. The result shows that decolorization is high at high acidic medium and then decreases when the pH of the solution increases. The decolorization reaches maximum at pH 4 and then decreases progressively up to pH 10. Hence, the pH 4 is assumed as optimum pH and is used for further analysis.

4.2. Effect of catalyst concentration

The impact of catalyst concentration on the removal of MB dye was tested using ZnO catalyst concentrations from 0.05 to 2 g/50 ml in 25 ppm MB dye solution at pH 4. The change in decolorization can be explained by the availability of number of surface active sites and the penetration of UV light into the dye solution. The results are displayed in Fig. 6; the figure clearly shows that the decolorization reaches maximum at 0.1 g/50 ml and increasing catalyst concentration more than 0.1 g/50 ml results in the decrease in decolorization. The maximum decolorization at 0.1 g/50 ml may be due to the presence of large number of ZnO nanoparticles for effective decolorization or enhanced active surface area. Hence large number of photons are absorbed by the catalyst surface and the dye solution. The reduced decolorization at higher catalyst concentration (more than 0.1 g/50 ml) may be due to the aggregation of ZnO nanoparticles. The aggregation of nanoparticles leads to the increase in scattering effect and, thereby decreases the active sites. Due to this UV light penetration decreased at higher catalyst concentrations. The same experimental procedure was followed for 50 ppm dye concentration. The obtained results are similar to 25 ppm dye concentration. Hence, 0.1 g/50 ml ZnO photocatalyst is assumed as optimum catalyst load and is used for further analysis.

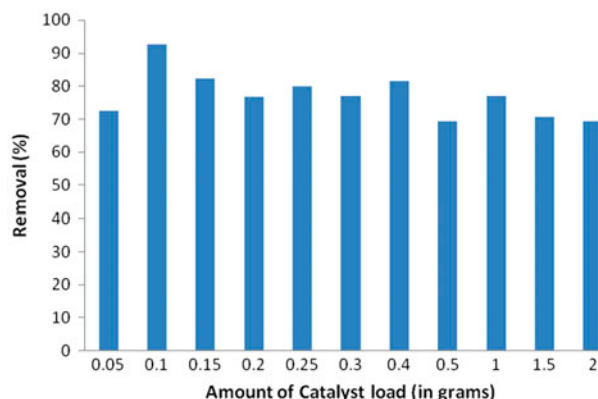


Fig. 6. Effect of catalyst loading on the photodegradation of MB.

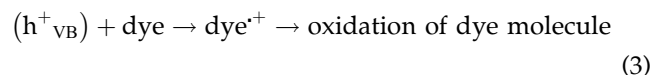
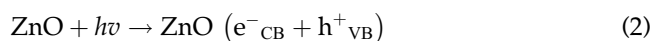
4.3. Effect of UV irradiation time

The photocatalytic decolorization of MB dye was carried out using the optimized pH (pH 4) and catalyst dosage (0.1 g/50 ml) for 25 and 50 ppm MB dye solutions. The obtained results are displayed in Fig. 7. The result shows that when the concentration of dye solution increases, the decolorization gets decreased. For both concentrations (25 and 50 ppm), the photodecolorization is maximum at 5 h UV irradiation. At 5 h light irradiation, the decolorization reaches 90% for 25 ppm and 70.8% for 50 ppm solution. The reduction of photocatalytic activity at higher concentration may be the reduced path length of photons into the higher concentrations and reverse is for the lower concentrations.

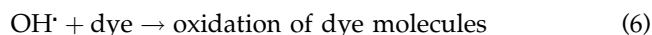
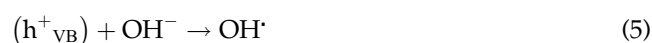
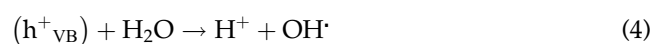
The obtained result is in contrast to the analysis carried out for the absence of UV light. For the absence of UV light the color degradation is only 6.5%, whereas no color removal for the absence of ZnO catalyst even for 5 h UV light irradiation. The obtained results are similar to the results reported by Shobana and Swaminathan for the photodegradation of AR18 [22].

According to the previously published literatures [23], we have proposed a mechanism for the enhanced photocatalytic activity of ZnO nanocrystals. The power of the semiconductor to act as a sensitizer and to enhance the photodegradation of the dye is based on their electronic structure with filled valence bond and empty conduction bond. The semiconductor photoexcitation instigated the photocatalyzed decolorization of dye in solution and it leaves the catalyst surface with a strong oxidative potential of an electron-hole pair (h^+_{VB}) which is shown in Eq. (2). When the photocatalyst was irradiated with higher energy photons, it allows the oxidation of the dye molecule in

a direct manner to the reactive intermediates, and given in Eq. (3).



The hydroxyl radical ($\text{OH}\cdot$), the exceptionally strong and a nonselective oxidant, which is formed either by decomposition of water (Eq. 4) or by the reaction of electron-hole along with hydroxyl ion (OH^-) given in (Eq. 5).



The hydroxyl radical and hydroxyl ions are responsible for degradation and decolorization of dye molecule (Eq. 6) [24]. It leads to the mineralization of MB.

5. Conclusion

ZnO nanocrystals have been synthesized by wet chemical method using different molarity concentrations. The synthesized nanocrystals are annealed at three different temperatures such as 250, 350, and 450°C. The grain size has been observed to decrease with the increase in molarity concentrations. The optical band gap has been observed to decrease with the increase in annealing temperature and increase with the increase in molarity concentrations. The impact of catalyst concentration, pH, and irradiation time on the removal of MB dye was tested using the synthesized ZnO nanocrystals. The results reveal that the decolorization is good at pH 4.

References

- [1] L.N. Zhang, L.T. Yan, X.D. Ai, T.X. Li, C.A. Dai, Preparation of a hybrid polymer solar cell based on MEH-PPV/ZnO nanorods, *J. Mater. Sci. Mater. Electron.* 24 (2013) 452–456.
- [2] P. Yang, X. Xiao, Y. Li, Y. Ding, P. Qiang, X. Tan, W. Mai, Z. Lin, W. Wu, T. Li, H. Jin, P. Liu, J. Zhou, C.P. Wong, Z.L. Wang, Hydrogenated ZnO core-shell nanocables for flexible supercapacitors and self-powered systems, *ACS Nano.* 7 (2013) 2617–2626.

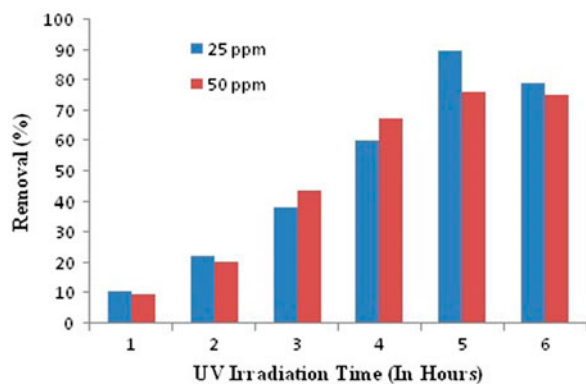


Fig. 7. Effect of irradiation time on the photodegradation of MB.

- [3] P. Yang, H. Yan, S. Mao, R. Russo, J. Johnson, R. Saykally, N. Morris, J. Pham, R. He, H.J. Choi, Controlled growth of ZnO nanowires and their optical properties, *Adv. Funct. Mater.* 12 (2002) 323–331.
- [4] M.H. Huang, S. Mao, H. Feick, H. Yan, Y. Wu, H. Kind, E. Weber, R. Russo, P. Yang, Room-temperature ultraviolet nanowire nanolasers, *Science* 292 (2001) 1897–1899.
- [5] T.S. Senthil, A.Y. Kim, N. Muthukumarasamy, M. Kang, Improved performance of dye sensitized ZnO nanorod solar cells prepared using TiO₂ seed layer, *J. Sol-Gel Sci. Technol.* 67 (2013) 420–427.
- [6] C. Hariharan, Photocatalytic degradation of organic contaminants in water by ZnO nanoparticles: Revisited, *Appl. Catal. A: Gen.* 304 (2006) 55–61.
- [7] L. Zhang, L. Du, X. Cai, X. Yu, D. Zhang, L. Liang, P. Yang, X. Xing, W. Mai, S. Tan, Y. Gu, J. Song, Role of graphene in great enhancement of photocatalytic activity of ZnO nanoparticle-graphene hybrids, *Phys. E* 47 (2013) 279–284.
- [8] Z.L. Wang, Progress in piezotronics and piezophototronics, *Adv. Mater.* 24 (2012) 4632–4646.
- [9] Z. Liang, X. Cai, S. Tan, P. Yang, L. Zhang, X. Yu, K. Chen, H. Zhu, P. Liu, W. Mai, Fabrication of n-type ZnO nanowire/graphene/p-type silicon hybrid structures and electrical properties of heterojunctions, *Phys. Chem. Chem. Phys.* 14 (2012) 16111–16114.
- [10] X. Xiao, L. Yuan, J. Zhong, T. Ding, Y. Liu, Z. Cai, Y. Rong, H. Han, J. Zhou, Z.L. Wang, High-strain sensors based on ZnO nanowire/polystyrene hybridized flexible films, *Adv. Mater.* 23 (2011) 5440–5444.
- [11] W. Mai, Z. Liang, L. Zhang, X. Yu, P. Liu, H. Zhu, X. Cai, S. Tan, Strain sensing mechanism of the fabricated ZnO nanowire-polymer composite strain sensors, *Chem. Phys. Lett.* 538 (2012) 99–101.
- [12] T.S. Senthil, A.Y. Kim, N. Muthukumarasamy, M. Kang, Effect of bath temperature on the performance of ZnO nanorod-based thin film solar cells, *J. Nanopart. Res.* 15 (2013) 1926-1–1926-9.
- [13] P. Yang, K. Wang, Z. Liang, W. Mai, C.X. Wang, W. Xie, P. Liu, L. Zhang, X. Cai, S. Tan, J. Song, Enhanced wettability performance of ultrathin ZnO nanotubes by coupling morphology and size effects, *Nanoscale* 4 (2012) 5755–5760.
- [14] Z. Li, X. Huang, J. Liu, Y. Li, G. Li, Morphology control and transition of ZnO nanorod arrays by a simple hydrothermal method, *Mater. Lett.* 62 (2008) 1503–1506.
- [15] C. Jia, X. Zhang, Y. Chen, Y. Su, Q. Zhou, M. Xin, Y. Lv, W. Kong, Liquid phase epitaxial growth and optical property of flower-like ZnO nanosheets on Zinc foil, *Appl. Surf. Sci.* 254 (2008) 2331–2335.
- [16] K. Haga, T. Suzuki, Y. Kashiwaba, H. Watanabe, B.P. Zhang, Y. Segawa, High-quality ZnO films prepared on Si wafers by low-pressure MO-CVD, *Thin Solid Films* 433 (2003) 131–134.
- [17] J.H. Lee, K.H. Ko, B.O. Park, Electrical and optical properties of ZnO transparent conducting films by the sol-gel method, *J. Cryst. Growth.* 247 (2003) 119–125.
- [18] X. Jiang, F.L. Wong, M.K. Fung, S.T. Lee, Aluminum-doped zinc oxide films as transparent conductive electrode for organic light-emitting devices, *Appl. Phys. Lett.* 83 (2003) 1875–1877.
- [19] N. Audebrand, J.P. Auffrédic, D. Louër, X-ray diffraction study of the early stages of the growth of nanoscale zinc oxide crystallites obtained from thermal decomposition of four precursors. General concepts on precursor-dependent microstructural properties, *Chem. Mater.* 10 (1998) 2450–2461.
- [20] N.M. Ganesan, N. Muthukumarasamy, R. Balasundaraprabhu, T.S. Senthil, Photo catalytic degradation of methylene blue by Ag incorporated TiO₂ nanocrystals prepared at different pH conditions, *Optoelectron. Adv. Mat.* 8 (2014) 581–586.
- [21] T.S. Senthil, N. Muthukumarasamy, M. Kang, Applications of highly ordered paddle wheel like structured ZnO nanorods in dye sensitized solar cells, *Mater. Lett.* 102–103 (2013) 26–29.
- [22] N. Sobana, M. Swaminathan, The effect of operational parameters on the photocatalytic degradation of acid red 18 by ZnO, *Sep. Purif. Technol.* 56 (2007) 101–107.
- [23] K. Vignesh, R. Priyanka, R. Hariharan, M. Rajarajan, A. Suganthi, Fabrication of CdS and CuWO₄ modified TiO₂ nanoparticles and its photocatalytic activity under visible light irradiation, *J. Ind. Eng. Chem.* 20 (2014) 435–443.
- [24] S.K. Kansal, M. Singh, D. Sud, Studies on photodegradation of two commercial dyes in aqueous phase using different photocatalysts, *J. Hazard. Mater.* 141 (2007) 581–590.